Madrid García, JA.; Yahaghi, E.; Movafeghi, A. (2021). Improvement of the digital radiographic images of old paintings on wooden support through the anisotropic diffusion method. Journal of Cultural Heritage. (49):115-122. https://doi.org/10.1016/j.culher.2021.02.008

Improvement of the digital radiographic images of old paintings on wooden support through the anisotropic diffusion method

Jose A. Madrid Garcia[1], Effat Yahaghi[2*], Amir Movafeghi[3]

[1]University Institute for the Restoration of the Patrimony, Universitat Politècnica de València, Valencia, Spain

[2] Department of physics, Imam Khomeini International University, Qazvin, Iran

[3] Reactor and Nuclear Safety School, Nuclear Science and Technology Research Institute, Tehran, Iran.

Imam Khomeini International University

Qazvin, Iran,

E-mail: yahaghi@sci.ikiu.ac.ir

Fax: (+98) 281 3780040

Phone: (+98) 281 3780040

Submitted to:

Abstract: The main defect types of historic-artistic paintings on wood are ruptures, scratches, twisting and such which may be inflicted by environment conditions, insects, dust, and dirt as well as by physical damage. The exact localization of the defects and determination of their extent may be achieved using industrial radiography as a non-destructive testing method. The radiographs thus produced may suffer from blurriness mainly due to the inherent scattering of X-rays especially in the case of paintings on a wooden base and hindering therefore accurate detection of the size and shape of such defects. Image processing methods have been employed to reduce the blurriness of images leading to improved analysis of the images. In this study, an image processing method based on anisotropic diffusion with an automatic threshold level was applied to achieve improved outcomes. The reconstructed images of the implemented algorithm yielded sharper edges. Defects such as those due to xylophagous attack, the effect of the brushstrokes, superficial fissures, oxidation of the nails, and the different types of construction woods were better visualized than from the original image. The algorithm was shown to be useful by operators including painting conservators for their procedures.

Keywords: Improvement, digital radiography, paintings on wooden support, anisotropic diffusion method, xylophagous attack

1. Introduction

Modern paintings conservators work in multidisciplinary teams, examining information in collaboration between conservators, art historians, and physics scientists using the latest technical tools. The teams aim to achieve higher certainty in determining the authenticity of the masterpieces

and valuations as well as assessment of deterioration through studying the materials and the original techniques used in the creation of the painting.

Deterioration can result in different ways such as changes in ambient temperature, exposure to humidity, insect attacks, deposits of dust and dirt scratch, or corrosion of some elements. As well as the cause of the deterioration, quantification of the defects' dimensions is necessary for deciding the most effective treatment [1].

X-ray radiography is used widely as a powerful tool in the chain of preservation of cultural heritage objects aiding art historians, social scientists and conservators. Other non-destructive testing (NDT) techniques, such as Ultraviolet Photography, Infrared Photography or Infrared Reflecto-graphy, Scanning Electron Microscope (SEM) and Fourier Transform Infrared Spectroscopy (FTIR) are useful for providing microscopic and macroscopic object data but lack the ability of X-ray radiography in revealing hidden information below the surface of the object [1-2].

In 1896, Köning [3], presented for the first time his results in the characterization of painting using X-ray. Burroughs [4], and others [5] also utilized the technique to show that radiography is capable of providing precise information on paintings' alterations, classification of materials, as well as the revelation of the brushstrokes. Mucchi [6] presented applied the tool to formulate a standard approach to painting analysis by considering four categories, referred to as the Mucchi's semiotics of radiography: (i) state of conservation, (ii) the pictorial technique used by the artist, (iii) creative process, and (iv) the stylistic evaluation [6].

Since those early applications, X-ray radiography has proved the most powerful tool in solving significant cases such as when Macht et.al [7] solved the authentication problem of the Portrait of George Washington, which had incorrectly been attributed to Gilbert Stuart. Madeleine Hours-

Miedan [8] has published numerous findings including also on works by Leonardo [9], Poussin's [10], and Rembrandt [11]. The success of X-ray radiography as a tool has roots in the technique's ability to reveal information from below the surface of the objects including the internal elements [12] and for example the fragility of painstaking brushwork [13].

Conventionally, radiography film is used for the detection of the X-rays traversing the object. In more recent years, Digital Radiography (DR) has gained in popularity since it is capable of yielding higher quality and contrast images [15-17]. Digital radiography can be performed with detector systems based on CCD or CMOS technologies as well as with phosphor imaging plate in combination with specialized plate reading scanners referred to as computed radiography (CR). Radiography films still provided superior spatial resolution (almost 10 μm). Flat panels in DR and phosphor imaging plates in CR yield resolutions between 40 to 100μm but have a much greater dynamic range.

Paintings are usually radiographed using the X-rays with a tube voltage of between 20 and 100 kVolt in CR. However, since the interaction of X-ray with matter is related to the atomic number and thickness variations of the paints, with their thin low atomic number wooden support, the acquired radiographs do not offer sufficient contrast for visualization of specific features [18-19].

The additional challenge in X-ray radiography of paintings is often their sizes. Paintings are usually large necessitating radiographic support set-ups in specialized Radiographic Inspection Laboratories (RIL) such as the unit located at the University Institute for the Restoration of the Heritage of the Universitat Politècnica de València [20-21] where the images used in this study was obtained from.

The goal of this study was to optimize the imaging process to yield higher quality final images. However since usual means of image optimization such as X-ray grids could not be utilized, instead, image processing needed to be rigorously applied to achieve this goal. Image processing methods are broadly grouped into pixel (spatial domain) or frequencies (Fourier domain) or a combination method such as wavelets [12-13]. Each method has its own advantages and can improve specific components of the image. One of the most effective methods in this application is the anisotropic diffusion method, which is based on the gradient of images [12, 24-25]. This filter is capable of extracting the image gradient at four main directions that can then be used to calculate the conduction coefficient of diffusion. Through solving for the solution with iterations and setting of region boundaries, the sharpness of the edges can be preserved by de-blurring and denoising of images [26-27].

In this study, we applied an anisotropic diffusion method to radiographs of a set of paintings on wood, which was based on the gradient of the images and an automatic threshold level algorithm. The paintings were selected from the catalog of case studies of the Radiographic Inspection Laboratory (RIL), University Institute for the Restoration of the Heritage of the Universitat Politècnica de València. The purpose of the study was to extract the maximum structural and identification information of the damaged areas and to develop an optimized procedure.

2. Methods

2.1 Description of the selected artistic painting

Eight on wood paintings with different pathologies which made them suitable candidates for X-ray radiography were chosen, Table 1. The suitability of the paintings was assessed on their

thickness and their internal structures. Also, the set covered a wide expanse of art history from the 15th to the 17th century, which expanded the evolution of the pictorial techniques over this period.

Technical *prior* information of the paintings is critical for effective conservation work. For the selected set of paintings such information included (i) the position of the metal assemblies in *Saint Catherine of Alexandria* (Fig.1-a), *Saint Michael* (Fig.1-b), (ii) *The eternal father in the act of blessing* (Fig.1-c), (ii) condition of the retaining nails as well as the added sections in *Saint Sebastian* (Fig.1-d), (iii) detail of the defects in the painting by the xylophagous attacks in *Ecce Homo* (Fig.1-e), (iv) the internal elements and the detail of the brushstroke, and *ductus* in *The Descent from* (Fig.1-f), (v) the added supports and fissures, and very xylophages attack in *Portrait of a gentleman* (Fig. 1g), (vi) *Saint Augustine of Hippo* (Fig. 1h), which has a systematic study by Mucchi [6], used the X-ray -radiography as a comparative semiotic study. This piece is an example of transit the paintings on canvas, which was subsequently replaced with the linear support approximately in the 16th to 17th centuries.

1.1 The radiography procedure

Fig. 2 shows the setup used for the acquisition of the radiographic images. The X-ray unit employed in this study was the TRANXPORTIX 50 X-ray machine from General Electric® which had 3 kW output power, a focal spot size of 2.3 mm, and a total filtration of 2 mm of aluminum and provided a range of 20 kVolt to 110 kVolt potential. The X-ray detection system used was phosphor imaging plates in conjunction with the laser scanner CR 30-X digitizer by AGFA®. The CR scanner was capable of yielding images with 4096 × 4096 pixels. The collimator of the X-ray machine was equipped with a light source that aided radiation beam positioning. The maximum attainable spatial resolution was around 100 micron (10 pixels /mm) with the setup used in this

study. For implementing the radiography technique, the painting is placed between an X-ray source and a detector. The attenuated X-ray that depends not only on the physical thickness of the materials it passes through but also on their atomic numbers which is recorded in the detector. The X-ray potential and the source to film (or detector) distance (SFD) was varied to suit the dimensions of paintings, that is, for larger paintings, the SFD had to be set greater and therefore necessitated the setting of a higher X-ray potential or higher tube current for obtaining the same contrast levels for a larger field of view and also larger SFD. The X-ray exposure settings used for the imaging of different paintings are shown in Table 2.

The main goals of the radiography of the paintings [6] were an investigation into their conservation status, painting technique employed by the artist, the process used for their construction and the artists' stylistic assessment. From the conservation viewpoint, the study was seeking to determine the depth or amount of the fissures and the level of oxidation present in the metallic elements. The painting technique employed by the artist can yield information about pieces' chronologically and also the location and origin of the piece. This information can be extracted from the shape of the assemblies, the use of any intermediate fabric, and the level of absorption of the pigments in the brush strokes. These aspects of the paintings are of course interlinked and can be studied simultaneously using radiographic imaging. Detection of any underlying painting or the position of any added parts yields information about the piece's evolutionary process and may be the key to its authentication by the art historian.

Table 3 shows *a prior* knowledge of the nature of damages and deteriorations that exist in the selected set of paintings.

2.2 Anisotropic Diffusion Image Processing Method

The anisotropic diffusion method is an image diffusion process that increases the intra-region smoothness of the image whilst reducing its inter-region smoothness. Mathematically, the process may be written as:

$$\frac{\partial}{\partial t} I(x,t) = \nabla.(c(x,t)\nabla I(x,t)) \quad (1)$$

where $c(x,t)$ is the diffusion function and is a monotonically decreasing function of the image gradient magnitude. x is the image coordinate, t is the iteration step and $I(x,0)$ is the initial unprocessed image. For edge estimation to locate the region boundaries the gradient of intensity image is first obtained using:

$$E(x,t) = \nabla I(x,t) \quad (2)$$

Then, the conduction coefficient of diffusion is computed locally as a gradient magnitude of local image intensities:

$$c(x,t) = f(\left|\left|\nabla I(x,t)\right|\right|) \quad (3)$$

Proper selection of the function f, can preserve region boundaries and can sharpen the edges within the image. A decreasing continuous function could be selected as a diffusion function. Two functions for local computation of the conduction to satisfy selective edge smoothness and enhancement were presented:

$$c(x,t) = \exp\left(\frac{\left|\left|\nabla I(x,t)\right|\right|}{k}\right)$$

$$c(x,t) = 1 + \left(\frac{1}{\left|\left|\nabla I(x,t)\right|\right|}\right)^2 \quad (4)$$

The first function in equation (4) increases the high contrast edges over the low contrast edges whilst the second function increases wide regions over smaller regions; k is the diffusion coefficient. The differential form of equation (1) can be discretized as:

$$I_{i,j}^{t+1} = I_{i,j}^{t} + \eta(N_C \nabla_N I + S_C \nabla_S I + W_C \nabla_W I + E_C \nabla_E I) \quad (5)$$

where N_c, S_c, W_c, and E_c are conduction in the image coordinate system of *north, south, west, and east* directions respectively. i and j denote the pixel position in a discrete, two-dimensional (2-D) grid and t denotes discrete time steps (iterations). The constant η is a scalar that determines the rate of diffusion.

Whilst retaining the phase of the image information, a noise threshold needs to be determined to reduce its amplitude. For automated thresholding, the mean and variance in the amplitude response of the smallest scale filter at a specific orientation should first be estimated. It can be assumed that the noise is Gaussian and the amplitude part of the image at each scale has a Rayleigh distribution such that [15]:

$$\mathrm{R}(x) = \frac{\mathrm{x}}{\sigma_{\mathrm{g}}^2} \exp\left(\frac{-\mathrm{x}^2}{2\sigma_{\mathrm{g}}^2}\right) \quad (6)$$

The median and variance of the amplitude can be estimated using:

$$\mu_{\mathrm{r}} = \sigma_{\mathrm{g}} \sqrt{\frac{\pi}{2}}, \sigma_{\mathrm{r}}^2 = \frac{4-\pi}{2} \sigma_{\mathrm{g}}^2 \quad (7)$$

and the threshold can be determined using:

$$T = \mu_r + k\sigma_r \quad (8)$$

k is usually set between 2 and 3.

In this study, the evaluation of results was carried out by the human operator. That is, a competent operator evaluated the quality of the images by scoring the resolution of the defect regions in the range from 0 and 5 with the score of zero for unacceptable, 1 for very bad, 2-3 for acceptable, 4 for good and 5 for excellent. The percentage of confirmation of images was calculated as:

$$\text{Confirmation Percent} = \frac{\sum \text{Score}}{\text{Maximum score (number of experts} \times 5)} \times 100 \quad (9)$$

Results and discussion

The X-ray radiography technique was used to examine hidden designs, damaged regions, and to reveal the physical characteristics of the creation of valuable paintings. Table 1 lists the paintings imaged in this study with established damages, deteriorations, and stylistic known to exist for each piece presented in Table 3. The anisotropic diffusion method (ADM) was applied to the images to improve the quality of assessment of each piece. Fig. 3-a shows the original X-ray radiograph of painting *The eternal father in the act of blessing* of the entire piece; Fig. 3-b shows a magnified section of the same painting. At the low X-ray energies used for these exposures, the image exhibits high contrast due to the wide range of atomic numbers and thicknesses of the piece despite the unavoidable imaging noise. The identified features and characteristics for the piece are identified with an "X" in Table 3. Despite the fine detail arising from its high contrast, the image was

somewhat foggy. The anisotropic diffusion method was utilized with the dynamic noise threshold level to remove the fogginess. Once the four gradients were calculated for every pixel, the diffusion function, C, was calculated using Eq. 4.

Assuming the image noise could be adequately described by a Gaussian distribution, the amplitude response was expected to be a Rayleigh distribution and the magnitude of the threshold vector was calculated using Eq. 8. The threshold level was then applied to the two image components and the processed image was reconstructed. Fig. 3-c and Fig. 3-d show the reconstructed images of the original radiographs. It can be seen that the application of the anisotropic diffusion algorithm and the thresholding method has removed the foggy components effectively, yielding clearer and sharper visualization of the content of the painting. As expected, details of some of the items were better visualized after contrast enhancement, including for example details of the construction, the damaged region in the supporting wood i.e. the xylophagous attack regions, and the use of the piece of cloth that had been placed as reinforcement between the two wooden boards.

Figs. 5 and 6 relate to the radiographic images of two painting *Saint Michael* and *Saint Catherine of Alexandria*. The internal construction as well as the damaged parts are apparent in both of the original radiographs, Fig. 5-a and Fig. 6-a. Of siginficance were the xylophagous attacks, low image contrasts of the brushstrokes, the superficial fissures, the extent of the oxidation of the nails, the different types of wood used in the construction and the fabric underpaintings.

Fig. 5-b and 6-b show the reconstructed images with the enhanced visualisation. The large and small cracks on the wood and the location of connecting nails were more clearly visible on the reconstructed images compared to the original images. The type of wood used with different grain patterns was more distinguishable on the processed images. Together with information relating to

the types of cut, as well as improved determination of the origin of the pieces, more informed and effective decisions could be made in any intervention processes.

The original and the reconstructed images of the *Saint Sebastian* painting are shown in Fig. 7-a and b where damaged regions including several cracks, splits and holes on the wood were revealed but the reconstructed images were found to be sharper. The xylophagous attack regions, the different types of wood used and the construction, the low quality of the contrasts of the brushstroke are also revealed. However, image contrast is enhanced after the application of the anisotropic method. The state of the wooden supports at the joints of the parts is also better visualized in the reconstructed image. Particular attention will be paid to the fissure that is masked in the upper right corner in the stucco area and the real extension of the oxide present in the nails that hold the added parts to both sides of the piece. Where the nails are inside the original wood appear to be less damaged.

Fig. 8-a,b and Fig. 8-c,d show the original and the reconstructed images of *The Descent from the Cross* paintings. The xylophagous attacks, low quality of the contrasts of the brushstrokes, the superficial fissures, the oxide of the nails region, and the different types of woods were better visualized on the reconstructed image.

The radiographs of the *Ecce Homo* painting are show in Fig. 9-a. This piece had suffered extensive xylophagous attacks resulting in widespread cavities. The full extent of the damage is more clearly visible on the reconstructed image. The low quality of the contrasts of the brushstrokes was distinguished better and the underlayer decorations such as the nimbus that appear around the head, which could not be visualized clearly on the original radiograph were more visible in the reconstructed image.

On the image of the *Portrait of a gentleman* painting (Fig. 10-a,c), the effects of xylophagous attacks, low quality of the contrasts of the brushstrokes and the superficial fissures were well visualized. On the reconstructed image (Fig. 10-b,d), these areas of damage and the construction detail were more recognizable due to the sharper edges. The reconstructed image gives a better quality and detail in those brushstrokes where the presence of a higher atomic number additive pigment is suggested.

The last of the images that were analysed was that of the *Saint Augustine of Hippo* painting (Fig. 11-a) where xylophagous attacks within the panels as well as the woodworking style were revealed (Fig. 11-c); once better visualization is achieved by the reconstructed images (Fig. 11-d).

The most interesting feature revealed within the images was the existence of another painting in the altarpiece under the layer visible to the naked eye. The reason for the re-usage of the base was not known but not a total surprise since *Saint Monica* was an early Christian saint and the mother of *St. Augustine of Hippo*, and for this reason, we find them represented in many other altarpieces. What was striking was the position of the latent figure, which appears inverted, pointing to the reusing of the base material. This discovery could chronical the evolution towards the use of fabric as a base for painting within the 17th century. If true, quite possibly the painter worked the fabrics on one side and then transferred it to the wooden support. From the perspective of this study however, was the higher capability of reconstructed images for visualization of such features.

With a view to the quantification of the improvement in visualization using r X-ray images, the pairs of original and reconstructed images were presented to two experienced radiographers and a conservator who were asked to score each pair for the revelation of their construction, damages

and defects regions. Table 4 shows the outcome of the analysis as the percentage of the average of operators' scores for the photographs, radiographs, and their reconstructed images using Eq. (9).

The outcome of this analysis showed that the reconstructed images were more effective for visualization in the damaged and xylophagous attacked regions and consistently provided better visualization of the designs. Also, whilst the broken regions and the damages of the wooden support were hard to distinguish using their photographs, they were effectively detected using the X-ray images. The operators also indicated their higher scores for the reconstructed images was due to the sharpness of the features in these images.

It should be noted that the run time for the anisotropic method algorithm on a core i7 personal computer with 8 GB RAM was about 60 seconds for 1000 pixels by 1334 pixels radiographic images.

4. Conclusion

The effectiveness of X-ray radiography for visualization of hidden construction detail, defects and damage of painting on wood has been reconfirmed. The improvement in revealing the inner construction of wooden paintings as well as defect detectability offered by the application of the anisotropic diffusion method as opposed to the original images alone has been demonstrated. The operator analysis has shown that the reconstruction images reveal more useful data in the damaged regions which would prove invaluable in restoration procedures where localisation of internal features and defects would be pivital to successful outcomes.

References

1. Bergmann U, Knox KT. Pseudo-color enhanced x-ray fluorescence imaging of the Archimedes Palimpsest. In: Berkner K, Likforman-Sulem L, editors. 2009. p. 724702. http://proceedings.spiedigitallibrary.org/proceeding.aspx?doi=10.1117/12.806053
2. Emilio Marengo a, Marcello Manfredi a, Orfeo Zerbinati a, Elisa Robotti a, Eleonora Mazzucco a, Fabio Gosetti a, Greg Bearman b, Fenella France c, Pnina Shor d, Development of a technique based on multi-spectral imaging for monitoring the conservation of cultural heritage objects, Analytica Chimica Acta, Volume 706, Issue 2, 14 November 2011, Pages 229-237 https://doi.org/10.1016/j.aca.2011.08.
3. Köning, W. (1896). 14 Photographien mit Röntgen-Strahlen aufgenommen im Physikalischen Verein zu Frankfurt a. M. Leipzig: Johann Ambrosius Barth.
4. Burroughs, A. (1938). Art criticism from a laboratory. Boston: Brown and Company.
5. Köning, W. (1896). 14 Photographien mit Röntgen-Strahlen aufgenommen im Physikalischen Verein zu Frankfurt a. M. Leipzig: Johann Ambrosius Barth.
6. Mucchi, L., & Bertuzzi, A. (1983). Nella profondità dei dipinti. La radiografia nell`indagine pittorica. Milan: Ed. Electa.
7. Hours-Miedan, M. (1964). Les secrets des chefs-d`oeuvre. L`oeuvre d`art est matière avant d`être message. Paris: Èditions Robert Laffont.
8. Hours-Miedan, M. (1952). La radiographie des tableux de Léonard de Vinci, Revue des Arts, 4, 227─235.
9. Hours-Miedan, M. (1960). Nicolas Poussin (1594-1665). Etude radiographique au Laboratorie du Musée du Louvre. Bulletin du laboratoire du Musée du Louvre, 5, 3-37.

10. Hours-Miedan, M. (1961). Rembrandt. Obsevations et préséntation des radiographies exécutées d´après les portraits et compositions du Musée du Louvre. Bulletin du laboratoire du Musée du Louvre, 6, 3-43.
11. Van Asperen de Boer, J., Van Schoute, R., Garrido, C., & Cabrera, J. Mª. (1983). Algunas cuestiones técnicas del «Descendimiento de la Cruz» de Roger van der Weyden, Boletín del Museo del Prado, 4(10), 39-50.
12. Garrido, C., & Hollanders-Favart, D. (1984). Las pinturas del «Grupo Memling» en el Museo del Prado: el dibujo sub-yacente y otros aspectos técnicos, Boletín del Museo del Prado, 5(15), 151─171
13. Martinez, T.D., Madrid, J.A., & Melchor, J.M., , Estudio preliminar de los materiales férreos de la villa romana de Sant Gregori (Burriana-Castellón) mediante RX, Jornades d'Arqueologia de la Comunitat Valenciana, 2013-2015 (2018), pp. 179-190.
14. Schalm, O., Vanbiervliet, L., Willems, P., & De Schepper P., Radiography of paintings: Limitations of transmission radiography and exploration of emission radiography using phosphor imaging plates, Studies in Conservation, 2013, Volume 59, 2014 - Issue 1.
15. Žemlička, J., Jakůbek, J., Dudák, J., Hradilová, J., &Trmalová O., X-ray radiography of painting with high resolution I. testing and measurements with large area pixels, Proceedings of the 5th Interdisciplinary Conference of ALMA, 20.–21. 11. 2014.
16. Yusà, D.J., Atienza B.D., & Madrid, J.A., Review of the work of Antonio Bisquert carried out in the city of Teruel through radiographic analysis and characterization of materials by SEM / EDX, Ge-Conservacion 1(16):6-22 December 2019.
17. Tonazzini, A., Salerno, E., Abdel-Salam Z,A., Harith, M.A., Marras, L., Botto, A., Campanella, B., d, Stefano Legnaioli d, Stefano Pagnotta d, Francesco Poggialini d

Vincenzo Palleschi, Analytical and mathematical methods for revealing hidden details in ancient manuscripts and paintings: A review, Journal of Advanced Research, Vol. 17, 2019, Pages 31-42, https://doi.org/10.1016/j.jare.2019.01.003.

18. Poulopoulos, P. , Pamplona, M., Richter, L., & Cwiertnia, E., Technological Study of the Decoration on an Erard Harp from 1818, Studies in Conservation, 2020, 65:2, 86-102, DOI: 10.1080/00393630.2019.1622317
19. Kawohl B. From Mumford-Shah to Perona-Malik in image processing", Math.Methods Appl. Sci. 2004; 27(15), 1803–1814 .
20. Madrid, J.A., 'Use of telemetry x-ray techniques in large-size pictorial works', in Ge-conservation, 5 (2013) 101−109.
21. Madrid, J.A., 'Dos décadas de inspección radiográfica en España: retrospectiva y horizontes futuros en un contexto de cambio tecnológico', in Intervención, 10 (2014) 87−95.
22. Caio A.PalmaFábio A.M.Cappabianco Jaime S.Ide, Paulo A.V. Miranda, Anisotropic Diffusion Filtering Operation and Limitations - Magnetic Resonance Imaging Evaluation, IFAC Proceedings Volumes, Volume 47, Issue 3, 2014, Pages 3887-3892, https://doi.org/10.3182/20140824-6-ZA-1003.02347
23. Mikula K. and Ramarosy N. Semi-implicit finite volume scheme for solving nonlinear diffusion equations in image processing". Numer. Math. 2001; 89(3), 561–590.J. Oh, S. Choi, Selective generation of Gabor features for fast face recognition on mobile devices. Pattern Recognition Letters, 34, 2013 .
24. Krissian, K., & Aja-Fernandez, S., Noise-Driven Anisotropic Diffusion Filtering of MRI IEEE Transactions on Image Processing, 18 (10) (2009), pp. 2265-2274 .

25. Chourmouzios Tsiotsios, Maria Petrou, On the choice of the parameters for anisotropic diffusion in image processing, Pattern Recognition, 46 (5) (2013), pp. 1369-1381 .
26. Voci, F., Eiho, S., Sugimoto, N., & Sekibuchi, H., Estimating the gradient in the Perona-Malik equation, Signal Processing Magazine, IEEE, 21 (3) (2004), pp. 39-65
27. Kovesi, P., Phase Preserving Denoising of Images. The Australian Pattern Recognition Society Conference: DICTA'99. Perth WA. pp 212-217 (December1999). http://www.cs.uwa.edu.au/pub/robvis/papers/p/denoise.ps.gz.
28. Poldi, G., C.Villa, G., Dalla conservazione alla storia dell'arte. Riflettografia e analisi noninvasive per lo studio dei dipinti. Pisa: Edizioni della Normale. 2006.
29. Poulopoulos, P., Pamplona, M., Richter, L., & Cwiertnia, E., Technological Study of the Decoration on an Erard Harp from 1818, Studies in Conservation, 2020, 65:2, 86-102, DOI: 10.1080/00393630.2019.1622317
30. Kawohl, B., From Mumford-Shah to Perona-Malik in image processing", Math.Methods Appl. Sci. 2004; 27(15), 1803–1814.
31. Palma, C.A., Cappabianco, F.A.M., Ide, J.S., & Miranda, P.A.V., , Anisotropic Diffusion Filtering Operation and Limitations - Magnetic Resonance Imaging Evaluation, IFAC Proceedings Volumes, Volume 47, Issue 3, 2014, Pages 3887-3892, https://doi.org/10.3182/20140824-6-ZA-1003.02347
32. Mikula, K., & Ramarosy, N., Semi-implicit finite volume scheme for solving nonlinear diffusion equations in image processing". Numer. Math. 2001; 89(3), 561–590.J. Oh, S. Choi, Selective generation of Gabor features for fast face recognition on mobile devices. Pattern Recognition Letters, **34**, 2013.

33. Krissian, K., & Aja-Fernandez, S., Noise-Driven Anisotropic Diffusion Filtering of MRI IEEE Transactions on Image Processing, 18 (10) (2009), pp. 2265-2274

34. Tsiotsios, Ch., & Petrou, M., On the choice of the parameters for anisotropic diffusion in image processing, Pattern Recognition, 46 (5) 2013, pp. 1369-1381.

35. Voci, F., Eiho, S., Sugimoto, N., & Sekibuchi, H., Estimating the gradient in the Perona-Malik equation, Signal Processing Magazine, IEEE, 21 (3) 2004, pp. 39-65

36. Kovesi, P., Phase Preserving Denoising of Images. The Australian Pattern Recognition Society Conference: DICTA'99. Perth WA. pp 212-217 December1999. http://www.cs.uwa.edu.au/pub/robvis/papers/p/denoise.ps.gz.

Table 1. Paints technical sheet.

Title	* Ref.	Dimensions (cm)	Century	Origin / Authorship	Current Location
Saint Catherine of Alexandria	813	162 × 55 × 2	14th to 15th	Probably Santa Clara Convent. Teruel (Spain) Spanish painting of Catalan Aragonese school.	Bishopric of Teruel and Albarracín (Spain)
Saint Michael	814	164 × 56 × 2	14th to 15th	Probably Santa Clara Convent. Teruel (Spain) Spanish painting of Catalan Aragonese school.	Bishopric of Teruel and Albarracín (Spain)
The eternal father in the act of blessing	924	70 × 215 × 4(10)	15th	Origin not determined. The piece that crowns an altarpiece today disappeared. Work of art attributed to the circle of Pere Cabanes (Master of Artés), a painter documented in Valencia between 1472 and 1538.	Sacristy of the parish church of saints Juanes de Puçol (Spain)
Saint Sebastian	733	78,50 × 34,40 × 1,90	16th	Origin not determined. Spanish painting of the Valencian school. Piece attributed to Joan de Joanes (c. 1510-1579).	Private collection
The Descent from the Cross The Descent from the Cross	365	55 × 128 × 7,00	16th	Origin not determined. Spanish painting of the Valencian school. Predella of an altarpiece attributed to Fray Nicolás Borras (c. 1530-1610).	Private collection
Ecce Homo	791	44 × 30 × 0,80	16th	Origin not determined. Spanish painting of the Valencian school. Piece attributed to Fray Nicolás Borras (c. 1530-1610).	Private collection
Portrait of a gentleman	798	60 × 47,50 × 0,70	17th	Origin not determined. French painting by anonymous author.	Private collection
Saint Augustine of Hippo	514	90 × 50 × 1,20	17th	Sacristy of the San Martín Church, Teruel (Spain) The centerpiece of the Altarpiece of Saint Augustine, by Antonio Bisquert (c. 1590-1646).	Sacred Art Museum, Teruel (Spain)

* Reference number in the Catalog of Studies ─ Radiographic Inspection Laboratory

Table 2. Technical parameters of exposure to obtain radiographs

	Voltage (kVolt)	**Current (mA)**	**Exposure time* (seconds)**	**Source to Film distance (cm)**	****Nº rx***
Saint Catherine of Alexandria	57	20	3	390	12
Saint Michael	58	20	3	390	12
The eternal father in the act of blessing	50	80	3	490	22
Saint Sebastian	45	20	3	230	6
Ecce Homo	48	20	3	200	4
The Descent from the Cross The Descent from the Cross	50	80	3	300	10
Portrait of a gentleman	57	20	3	220	6
Saint Augustine of Hippo	59	20	3	340	8

* Exposure time in each of the radiographs.

** Nº rx*is the number of Shooting on the radiography.

Table 3. List of damages, deteriorations, and stylistic assessment present in the paintings.

	1.- Saint Catherine of Alexandria	*2.- Saint Michael*	*3.- The eternal father in the act of blessing*	*4.- Saint Sebastian*	*5.- Ecce Homo*	*6.- The Descent from the Cross*	*7.- Portrait of a gentleman*	*8.- Saint Augustine of Hippo*
Superficial fissures	X	X	X	X	X	X	X	
Crack and fine fracture	X	X	X	X	X	X	X	
Xylophagous attacks and damage of wood	X	X	X	X	X	X	X	X
Presence of rust of the metallic elements	X	X	X	X		X		
Different types of Woods	X	X	X	X		X		X
Low quality of the contrasts of the brushstrokes	X	X	X	X	X	X	X	
Use of fabric under the coat of paint	X	X	X	X				X
Presence of an underlying painting								X

Table 4. The result of opinions experts for the photographs, original radiography, and reconstructed images.

Feature	Photograph images	Original radiography	Reconstructed images
Superficial fissures	32%	80%	90%
Crack and fine fracture	35%	90%	95%
Xylophagous attacks and damage of wood	15%	85%	95%
Presence of the rust in the metallic elements	12%	90%	95%
Different types of woods	0%	100%	100%
Low quality of the contrasts of the brushstrokes	20%	87%	92%
Use of fabric under the coat of paint.	0%	90%	95%
xylophage attacks	30%	89%	97%
Presence of an underlying painting	0%	90%	95%

a

b

c

d

e

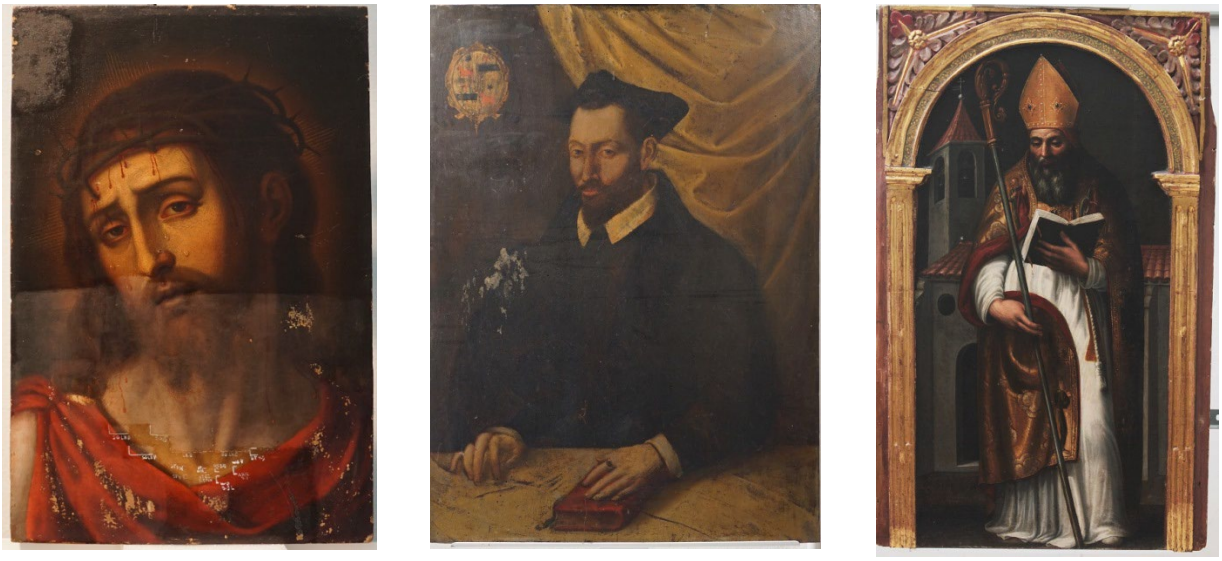

f g h

Fig.1. a) *Saint Catherine of Alexandria* (Ref.- 814), b) *Saint Michael* (Ref.- 813),c)*The eternal father in the act of blessing* (Ref.- 924), d) *Saint Sebastian* (Ref.- 733), e) *The Descent from the Cross* (Ref.- 365), f) *Ecce Homo* (Ref.- 791), g) *Portrait of a gentleman* (Ref.- 798) and h) *Saint Augustine of Hippo* (Ref.- 514).

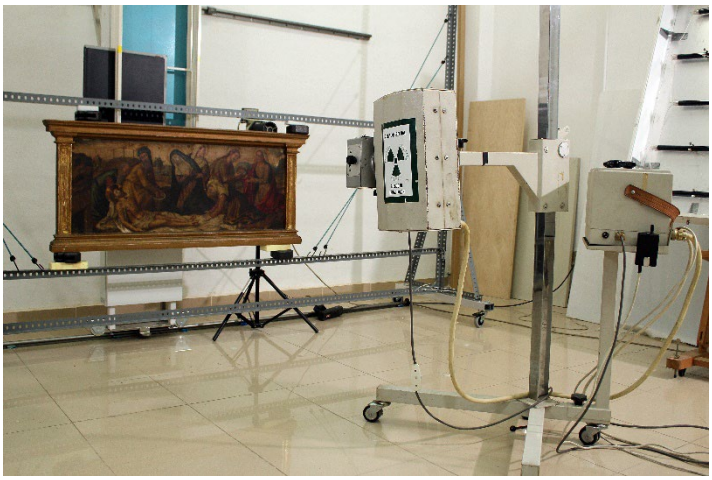

Fig. 2. The radiography set up.

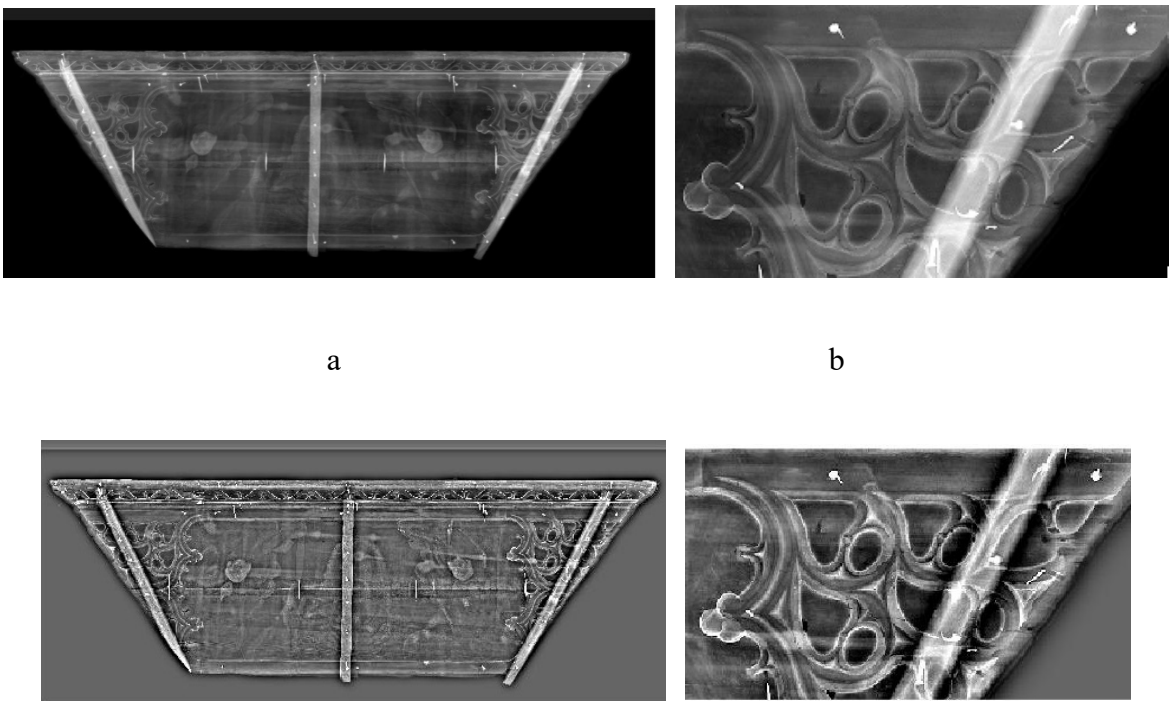

a b

c d

Fig.3 a and c) the radiography of *The eternal father in the act of blessing* and the reconstructed image by the anisotropic diffusion method b and d) the larger zoom of the marked zones.

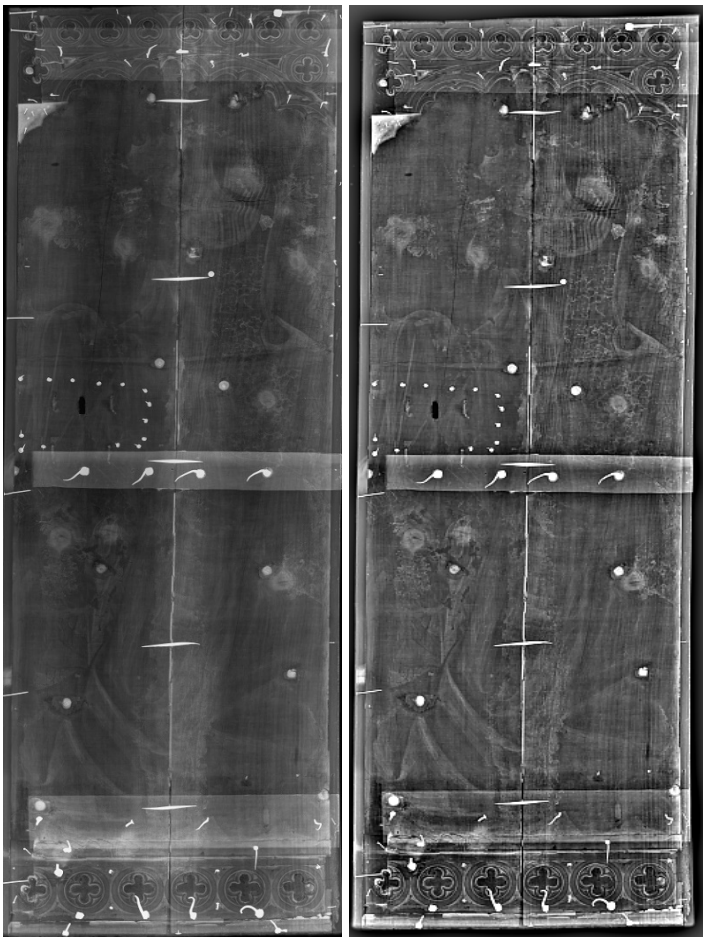

a b

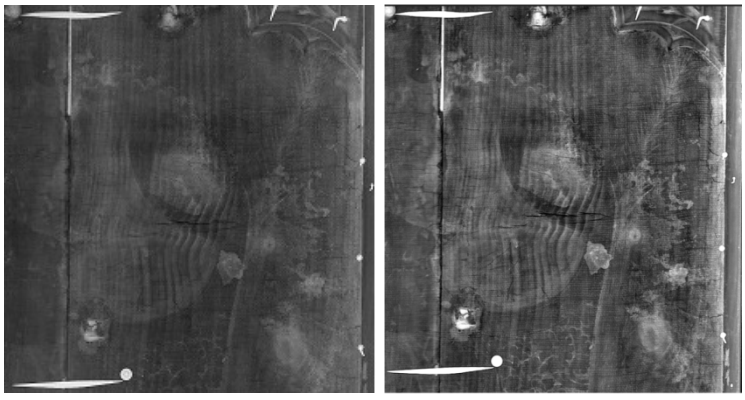

c d

Fig.5 a and c) the radiography of the *Saint Michael* painting and the reconstructed image by the anisotropic diffusion method b and d) the larger zoom of the marked zones.

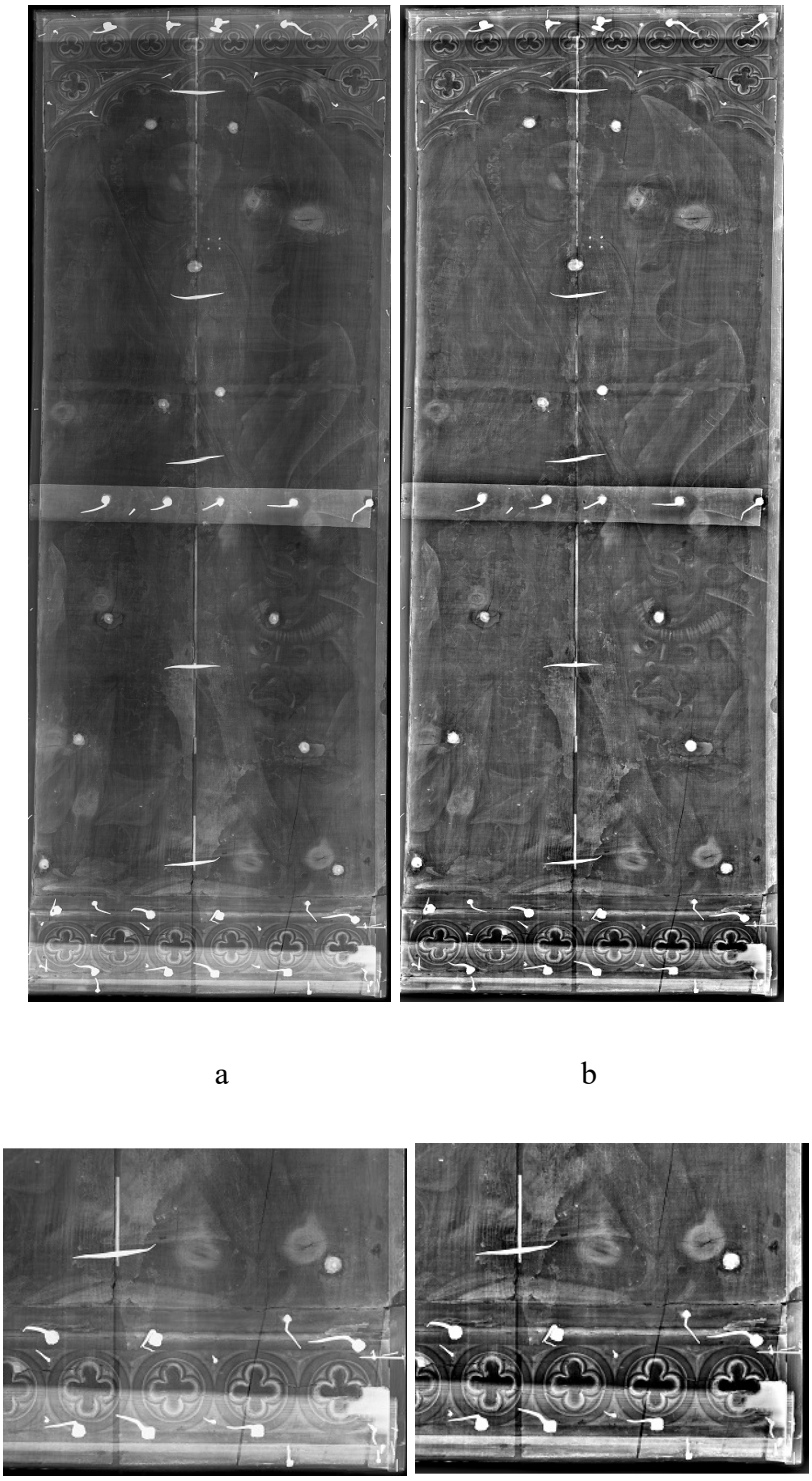

a b

c d

Fig.6 a and c) the radiography of the and *Saint Catherine of Alexandria* painting and the reconstructed image by the anisotropic diffusion method b and d) the larger zoom of the marked zones.

a b

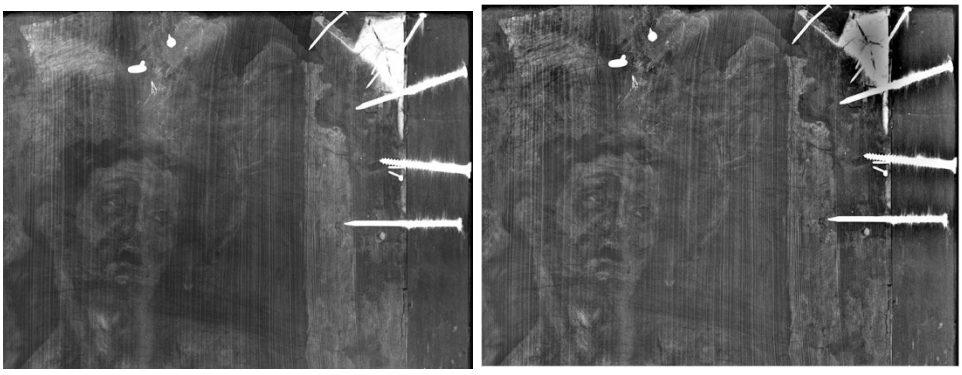

c d

Fig.7- a and c) the radiography of the *Saint Sebastian* painting and the reconstructed image by the anisotropic diffusion method b and d) the larger zoom of the marked zones.

a

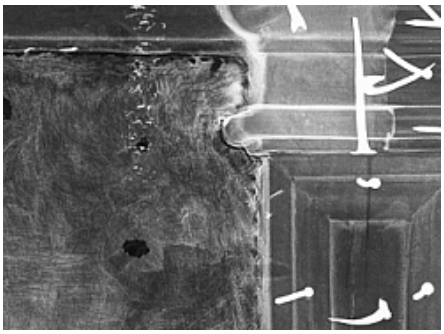

b

c

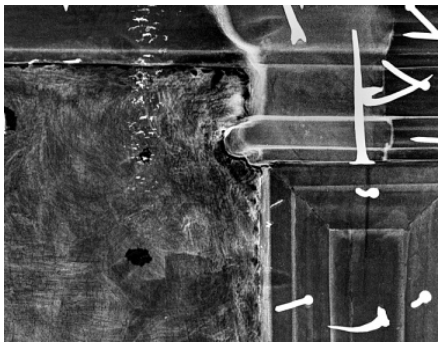

d

Fig.8 a and c) the radiography of *The Descent from the Cross*and the reconstructed image by the anisotropic diffusion method b and d) the larger zoom of the marked zones.

Fig.9 a) the radiography of the *Ecce Homo*portrait and b) the reconstructed image

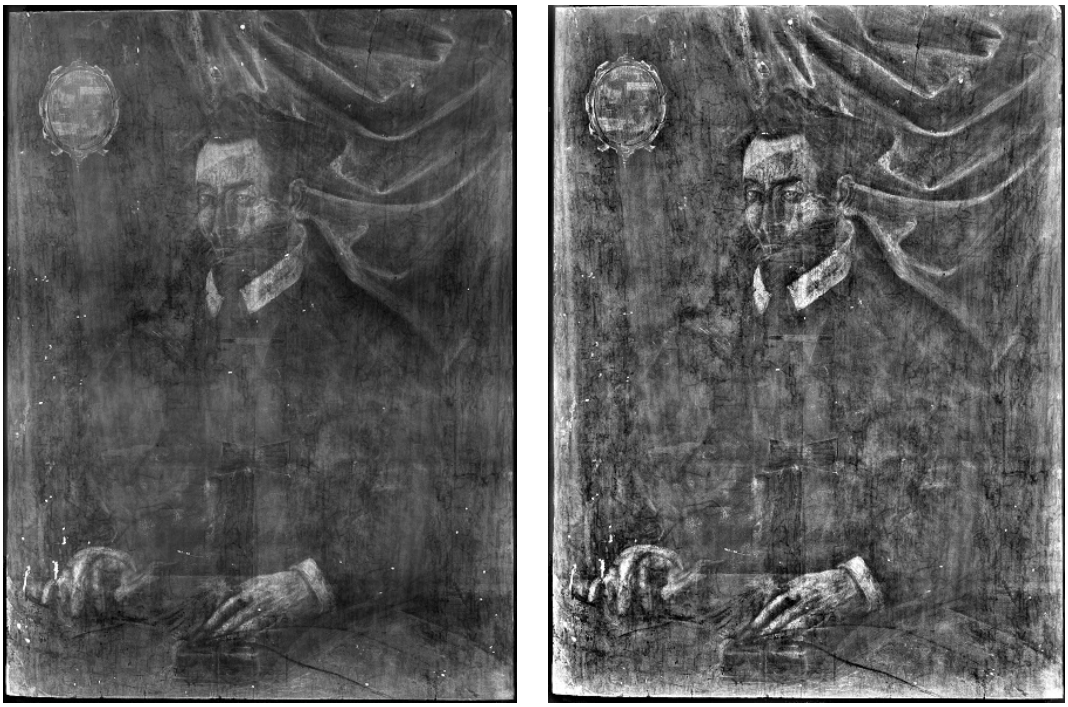

a b

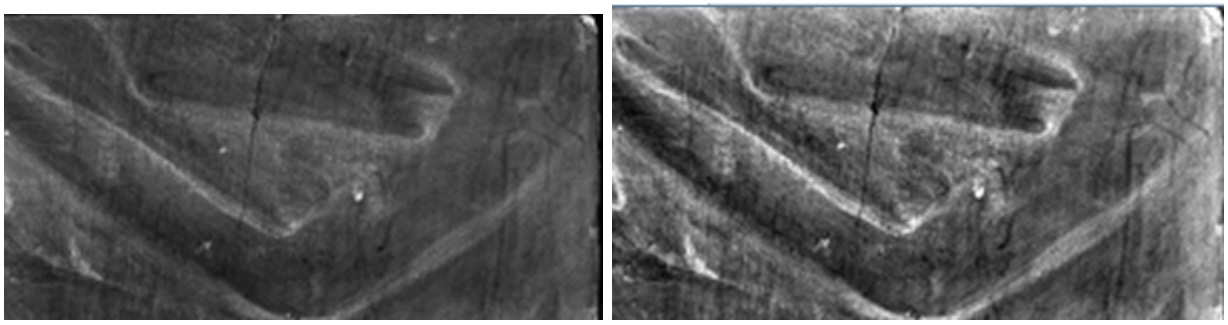

c d

Fig.10 a and c) the radiography of the *Portrait of a gentleman* and the reconstructed image by the anisotropic diffusion method b and d) the larger zoom of the marked zones.

a b

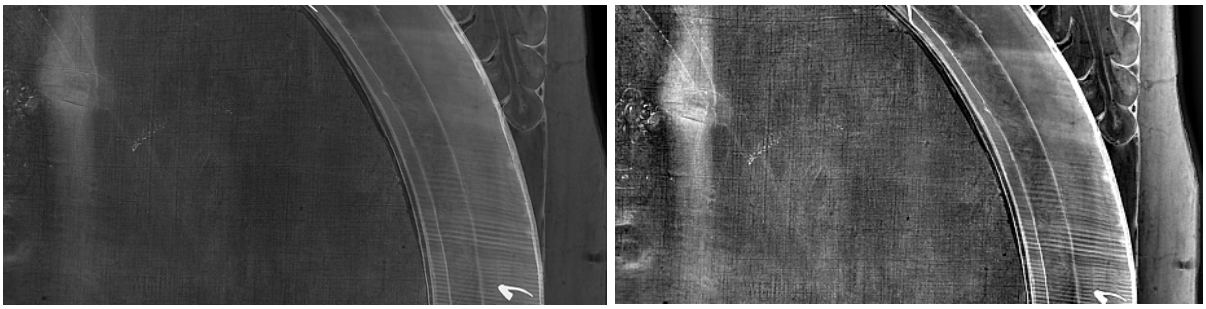

c d

Fig.11 a and c) the radiography of the *Saint Augustine of Hippo* painting and the reconstructed image by the anisotropic diffusion method b and d) the larger zoom of the marked zones.